Macromolecules

pubs.acs.org/Macromolecules

Article

Papain-Catalyzed, Sequence-Dependent Polymerization Yields Polypeptides Containing Periodic Histidine Residues

Kayo Terada, Taichi Kurita, Joan Gimenez-Dejoz, Hiroyasu Masunaga, Kousuke Tsuchiya,* and Keiji Numata*

Cite This: *Macromolecules* 2022, 55, 6992−7002

Read Online

ACCESS | Metrics & More | Article Recommendations | Supporting Information

ABSTRACT: His-containing polypeptides, including polyHis, are attractive materials due to the unique characteristics of the imidazole ring of the His residue. In particular, His-containing polypeptides with repetitive sequences have a variety of distinctive features based on their periodic structure. In this study, chemoenzymatic polymerization of ethyl ester monomers with sequences His, GlyHis, HisGly, and GlyHisGly with hydrophobic side chains on the imidazole ring was performed using papain as a catalyst. Sequence dependence in chemoenzymatic polymerization was observed for GlyHis- and HisGly-based monomers: GlyHis-based monomers did not undergo polymerization, whereas polymerization of HisGly-based monomers afforded polypeptides with a degree of polymerization from 6 to 38 and from 5 to 31 and a number-average degree of polymerization of 16.4 and 12.4 for poly(HisGly) and poly[His(Bu)Gly], respectively. The difference in polymerizability of these dipeptide monomers was supported by a docking simulation between these monomers and papain, where the ester group of the HisGly-based monomer was closer to the catalytic center of papain than that of the GlyHis-based monomer. Infrared spectroscopy and synchrotron wide-angle X-ray diffraction measurements indicated that poly(HisGly) formed a β-sheet structure whose crystallinity was 41.6%, whereas the other tripeptide-based polypeptides were more amorphous showing 19.6−30.7% of crystallinity. Poly(HisGly) exhibited the highest thermal stability among all of the polypeptides in the thermogravimetric analysis, reflecting the difference in the secondary structures.

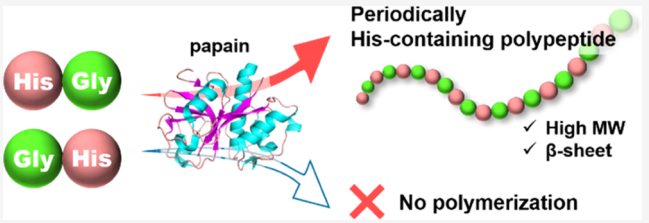

INTRODUCTION

Polypeptides and proteins, which are composed of amino acids with side chains varying in size, hydrophobicity, charge, and reactivity, have attracted great interest as biobased materials with useful physical, chemical, and biological properties.[1−6] These properties originate from the sequence of the amino acid residues and their higher-order structures. Polypeptide- and protein-based materials are considered promising alternatives to synthetic materials because they can be tailor-made by the selection and arrangement of amino acid residues.

There are 22 proteinogenic amino acids as well as nonproteinogenic amino acids, such as γ-aminobutyric acid (GABA), L-3,4-dihydroxyphenylalanine (DOPA), and hydroxyproline (Hyp). This diversity of constituent amino acids gives polypeptides and proteins a wide variety of structural and functional properties. Among 22 proteinogenic amino acids, histidine (His) is one of the most versatile because of the unique characteristics of the imidazole ring in its side chain, as follows: (i) the imidazole ring is aromatic, which leads to interaction with aromatic and cationic amino acid residues in polypeptides and proteins via $\pi-\pi$ and cation$-\pi$ interactions; (ii) the imidazole ring has a hydrogen-bond donor and acceptor, that is, a polar hydrogen atom and a basic nitrogen atom, respectively; (iii) the pK_a of the imidazole ring of His is approximately 6.1 and the protonation of the imidazole ring occurs near physiological pH; and (iv) the basic nitrogen atom in the imidazole ring has a lone pair that enables coordination with transition metals such as Ca, Ni, and Zn. The multiple interactions of His residues listed above contribute to the complicated and sophisticated features of polypeptides and proteins.[7−11] The His residue is often a key residue in the catalytic reactions of enzymes such as serine proteases and cysteine proteases.[12−15] In the catalytic triad of these proteases, the basic nitrogen atom of the His residue helps deprotonate hydroxy or thiol groups through His, which is the first step of the protease-catalyzed reaction.

Although His-containing polypeptides, including polyHis, are thus attractive materials, the synthesis of His-containing polypeptides is difficult and costly because the protection of the imidazole ring of His is necessary to prevent undesired coupling at the side chain in conventional synthetic methods.

Received: May 18, 2022
Revised: July 21, 2022
Published: August 8, 2022

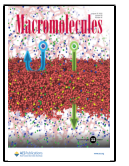

https://doi.org/10.1021/acs.macromol.2c01036
Macromolecules 2022, 55, 6992−7002

His-containing polypeptides with complicated amino acid sequences have been synthesized via solid-phase peptide synthesis (SPPS) and solution-phase peptide synthesis by sequential coupling chemistry using condensation reagents such as carbodiimide derivatives. The primary and higher-order structures of the resulting His-containing polypeptides give unique physiological functions performed by the His residues.[16−20] However, tedious stepwise reactions are necessary, which limits the available peptide length and large-scale production capable of huge supply for bulk material applications. Ring-opening polymerization (ROP) of amino acid *N*-carboxyanhydrides (NCAs) provides polyHis and its derivatives with random or block sequences.[21−24] This technique can precisely control molecular weight and construct special architectures such as block and graft polymers, but more complicated amino acid sequences are unattainable. Although the bulk-scale production of functional polypeptides with sophisticated insertion of His residues is highly desired for various applications, conventional synthetic methods all have disadvantages in large-scale production with well-defined sequential control. To overcome these issues, we are focusing on the utilization of chemoenzymatic polymerization.

As an eco-friendly synthetic method, chemoenzymatic polymerization should offer several advantages for the preparation of His-containing polypeptides. The chemoenzymatic polymerization of amino acid ester derivatives catalyzed by proteases has been developed as an alternative method to conventional synthetic methods such as SPPS and ROP of NCAs. In contrast to conventional methods, this technique does not require any side chain protection of the monomers, which allows for a facile and cost-effective synthesis of polypeptides.[25−31] Polymerization is performed in an environmentally benign aqueous system, and purification can be performed easily by washing precipitates with water regarding to water-insoluble polypeptides. Using di- or tripeptide esters as monomers, chemoenzymatic polymerization can afford periodic polypeptides that have previously been conventionally prepared by costly, time-consuming stepwise condensation methods using condensation agents.[32] Low-affinity natural amino acids for the enzyme, such as proline and valine, can be incorporated into the polypeptide sequence using a tripeptide ethyl ester in which the low-affinity residue is sandwiched between two alanine (Ala) or glycine (Gly) residues as monomers.[33] This technique is also applicable for the incorporation of unnatural amino acids with no specificity for enzymes, affording polypeptides containing α-aminoisobutyric acid (Aib) units, nylon units, or aromatic units, which have a similar structure to engineering plastics.[34−36]

The introduction of His residues into repetitive sequences imparts distinct physical and physiological properties to polypeptides depending on the periodic structures. For example, periodic polypeptides consisting of His and Lys residues were synthesized by SPPS followed by a chain extension reaction via terminal Cys residues for peptide carriers of DNA delivery.[37] The sequential variation of His-containing repetitive polypeptides displayed distinct diversity in their ability to bind to DNA. We recently reported the chemoenzymatic polymerization of the His-containing tripeptide ester GlyHis(Bu)Gly using papain to obtain the periodic His-containing polypeptide poly[GlyHis(Bu)Gly].[38] By post-modification of the imidazole ring with a butyl group followed by hydrolysis of the butyrate group, we converted it to the zwitterionic polypeptide poly[GlyHis^{zw}(Bu)Gly] having the imidazolium salt as a cationic component and the carboxylate as an anionic component, which exhibited the ability to dissociate the cellulose network due to the imidazolium-based zwitterionic structure, similar to ionic liquids. However, there are only a few reports on the chemoenzymatic synthesis of His-containing polypeptides, including the above-mentioned report, although it should be a valid approach for the preparation of His-containing polypeptides with the potential for their practical use.[39,40] Herein, we examined the chemoenzymatic polymerization of histidine derivatives to obtain polypeptides with various functionalities. Chemical characterization of the resulting His-containing polypeptides was performed by proton nuclear magnetic resonance (^{1}H NMR) spectroscopy and matrix-assisted laser desorption/ionization time-of-flight (MALDI-TOF) mass spectrometry. In addition, the secondary structure of the His-containing polypeptides was characterized by circular dichroism (CD), infrared spectroscopy (IR), and synchrotron wide-angle X-ray diffraction (WAXD) measurements.

EXPERIMENTAL SECTION

Materials. Papain (EC No. 3.4.22.2) was purchased from FUJIFILM Wako Pure Chemical Corporation (Osaka, Japan) and used as received. The activity was approximately 0.5 U g^{-1}, where one unit hydrolyzes 1 μmol *N*-benzoyl-DL-arginine *p*-nitroanilide per minute at pH 7.5 and 25 °C. *N*-*tert*-Butoxycarbonyl-L-histidine (Boc-His-OH) was purchased from Chemscene LLC (Monmouth Junction, NJ) and used without purification. The other amino acid derivatives and 1-(3-(dimethylamino)propyl)-3-ethylcarbodiimide (EDC) hydrochloride salt were purchased from Watanabe Chemical Industries Ltd. (Hiroshima, Japan) and used as received. Boc-HisGly-OEt, His(Bu)-Gly-OEt 2HCl salt, and GlyHis(Bu)Gly-OEt 2HCl salt were synthesized according to the literature.[38] Deuterated trifluoroacetic acid (TFA-*d*) was purchased from Sigma-Aldrich (St. Louis, MO). Deuterated chloroform (chloroform-*d*) and deuterated dimethyl sulfoxide (DMSO-d_6) were purchased from FUJIFILM Wako Pure Chemical Co. (Osaka, Japan). The other chemicals were purchased from Tokyo Chemical Industry Co., Ltd. (Tokyo, Japan) and used as received without purification unless otherwise noted.

General Procedure of Chemoenzymatic Polymerization of His-Derived Monomers. To a 10 mL glass tube equipped with a stir bar were added HisGly-OEt·2HCl (154 mg, 0.492 mmol) and 1 M phosphate buffer (PB, pH 8.0, 492 μL), and the mixture was stirred at 40 °C until the substrate was completely dissolved. Then, papain (24.6 mg) was added to this solution. The final concentrations of monomer and papain were 1.0 M and 50 mg mL^{-1}, respectively. The resulting mixture was stirred at 800 rpm and 40 °C for 2 h. After cooling to 25 °C, the precipitate was collected by centrifugation at 9000 rpm at 4 °C for 15 min. The crude product was washed with Milli-Q water and lyophilized to provide poly(HisGly) as a white solid. The yield was 41.4 mg (32%).

Analysis. *Fourier Transform Infrared (FT-IR) Spectroscopy.* The FT-IR spectra of the bulk samples were recorded on an IRPrestige-21 FT-IR spectrophotometer (Shimadzu Corporation, Kyoto, Japan) with a MIRacle A single-reflection attenuated total reflectance (ATR) unit using a Ge prism. The spectra from 700 to 4000 cm^{-1} were accumulated at 4 cm^{-1} resolution using 32 scans.

Nuclear Magnetic Resonance (NMR) Spectroscopy. The ^{1}H NMR spectra were recorded on a Bruker DPX-400 spectrometer (Karlsruhe, Germany) at 25 °C and 400 MHz. Chloroform-*d*, DMSO-d_6, or TFA-*d* was used as the solvent, and tetramethylsilane (TMS) served as an internal standard.

Matrix-Assisted Laser Desorption/Ionization Time-of-Flight Mass Spectroscopy (MALDI-TOF MS). MALDI-TOF mass spectroscopy analysis was conducted using an ultrafleXtreme MALDI-TOF spectrophotometer (Bruker Daltonics, Billerica, MA) operating in the

https://doi.org/10.1021/acs.macromol.2c01036
Macromolecules 2022, 55, 6992−7002

Scheme 1. Papain-Catalyzed Chemoenzymatic Polymerization of His-Containing Monomers

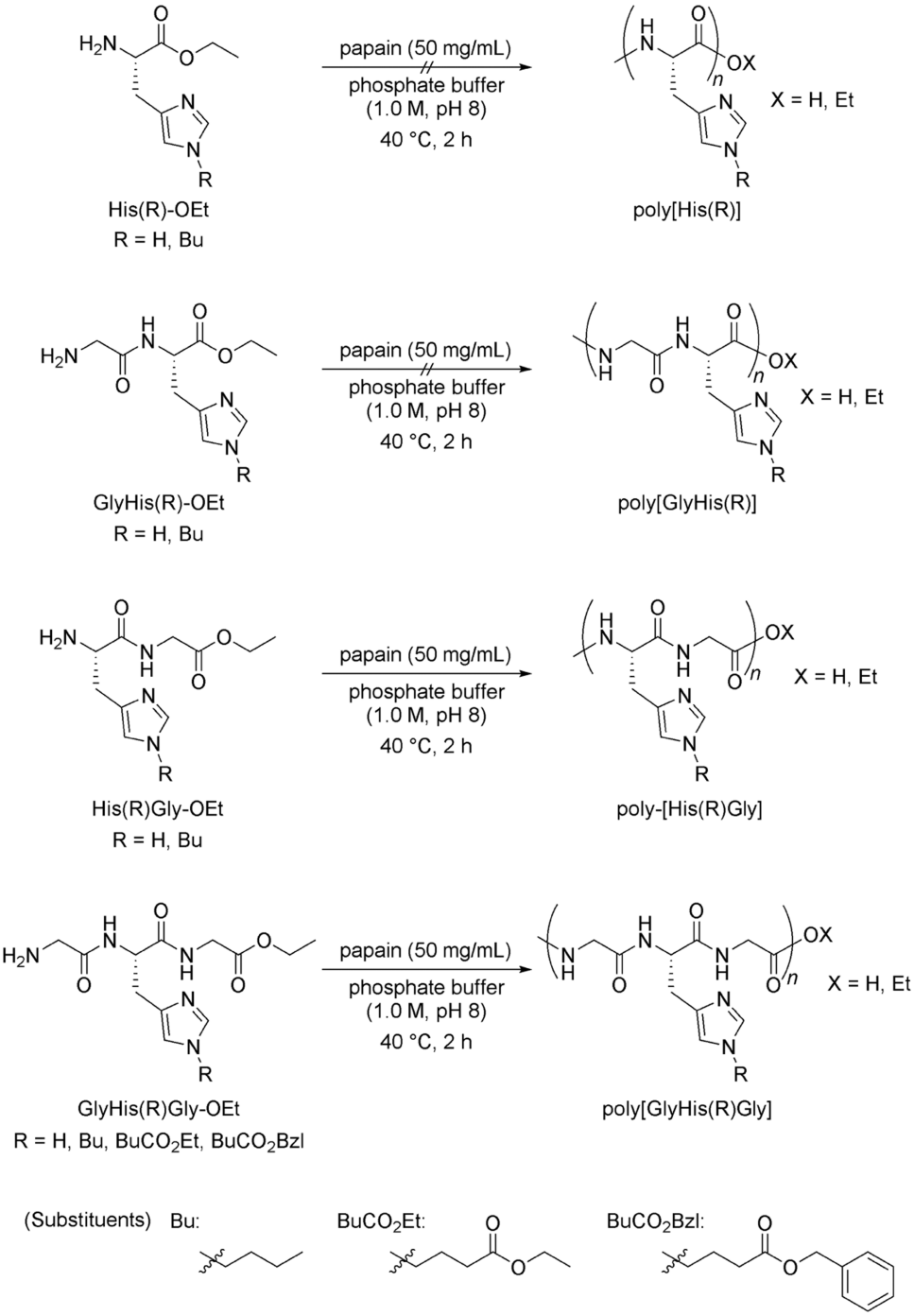

linear positive ion mode. The sample was dissolved in TFA or water containing 0.1% TFA and mixed with a solution of α-cyano-4-hydroxycinnamic acid (CHCA) in acetonitrile. The reaction solution forming no precipitate was purified with ultrafiltration using an Amicon Ultra unit (Merck, MWCO: 3 k, 9000*g*, 25 °C, 45 min) to remove the papain. The collected filtrate solution was desalted using Zip Tip (Merck, 0.6 μL, C_{18}) and then characterized by MALDI-TOF MS to identify the water-soluble product.

Wide-Angle X-ray Diffraction (WAXD) Measurements. The synchrotron WAXD measurements of bulk samples in the pellet form were performed on the BL05XU beamline (SPring-8, Harima, Japan) using X-ray energy of 15 keV (wavelength: 0.82 Å). The pellet was placed in a cell covered with a poly(ether ether ketone) (PEEK) film on the beamline and irradiated with X-rays for 1 s. The two-dimensional (2D) diffraction pattern was obtained after subtracting the background pattern of the PEEK film. The obtained 2D diffraction patterns were converted to one-dimensional (1D) profiles by azimuthal integration using Fit2D. The crystallinity was calculated from the area of the crystal peaks divided by the total area of the crystal peaks and the amorphous halo by fitting the Gaussian function using Origin Pro 2021 (OriginLab, Corp., Northampton, MA).

Thermogravimetric (TG) Analysis. The TG measurements were performed using a Mettler Toledo TGA/DSC 2 Star system (Greifensee, Switzerland). Samples (3 mg) were encapsulated in aluminum pans and heated under a nitrogen atmosphere from 30 to 500 °C at a heating rate of 20 °C min^{-1}. To remove the water completely, the temperature was held at 100 °C for 10 min before

https://doi.org/10.1021/acs.macromol.2c01036
Macromolecules 2022, 55, 6992−7002

Table 1. Chemoenzymatic Polymerization of His-Containing Monomers Catalyzed by Papain[a]

run	monomer	concn. (M)	yield[b] (%)	DP_{top}[c]	DP_{max}[d]	DP_n[e]
1	His-OEt	1.0	0			
2	His(Bu)-OEt	1.0	0			
3	GlyHis-OEt	1.0	0			
4	GlyHis(Bu)-OEt	1.0	0			
5	HisGly-OEt	1.0	32	9	39	17.4
6	His(Bu)Gly-OEt	1.0	28	11	35	12.4
7	GlyHisGly-OEt	1.0	57	6	29	
8	GlyHisGly-OEt	0.10	0			
9	GlyHis(Bu)Gly-OEt	0.10	62	6	20	
10	GlyHis($BuCO_2Et$)Gly-OEt	0.10	70	9	22	
11	GlyHis($BuCO_2Bzl$)Gly-OEt	0.10	54	3	10	

[a]Polymerization was carried out using monomer (HCl salt) and papain (50 mg mL^{-1}) in phosphate buffer (1 M, pH 8.0) at 40 °C for 2 h. [b]The precipitate was collected by centrifugation, washed with water, and lyophilized. [c]Degree of polymerization of the highest peak determined by MALDI-TOF MS. [d]Maximum degree of polymerization determined by MALDI-TOF MS. [e]Number-average degree of polymerization determined by ^1H NMR.

heating to 500 °C. The 5% degradation temperature (T_{d5}) was determined based on the weight after the removal of water at 100 °C.

Differential Scanning Calorimetry (DSC). DSC measurements were carried out on a Perkin-Elmer DSC 8500 (Perkin Elmer) equipped with a liquid nitrogen cooling accessory. DSC measurements were carried out by encapsulating 3−5 mg of sample in aluminum pans. The sample was first heated from 30 to 200 °C, cooled to −50 °C, and heated again to 200 °C. The heating and cooling rates were 20 and 100 °C min^{-1}, respectively.

Molecular Docking Simulations. All molecular docking studies were performed using docking program AutoDock Vina version 1.1.2.[41] For the protein molecule, the crystallographic structure of papain (PDB ID: 1ppn) solved at 1.6 Å resolution was used.[42] Before docking, all ligands and water molecules were removed from the PDB file. Polar hydrogens were added to ligands and receptors by using the Hydrogen module in AutoDock Tools version 1.5.6. Then, Gasteiger united atom partial charges and atom types were assigned, and PDBQT files were generated for AutoDock Vina docking. The protein molecule was kept rigid, while all of the torsional bonds in substrates were set free to rotate. A 15 Å docking box around the sulfur atom of Cys25 was defined. Images were prepared using PyMOL 1.8.5.

RESULTS AND DISCUSSION

Chemoenzymatic Synthesis of His-Containing Polypeptides Using Papain. We chose and synthesized His-containing ethyl ester monomers with sequences His, GlyHis, HisGly, and GlyHisGly for chemoenzymatic polymerization (Scheme 1). The monomers were synthesized according to Schemes S1−S6 and Figures S1−S19. Polymerization of monomers linked with butyl or butyrate groups (Bu, $BuCO_2Et$, or $BuCO_2Bzl$) to the imidazole ring of the His residue was also performed to examine the effect of the substituents. Similar to poly[GlyHis^{zw}(Bu)Gly], the butyl-linked imidazole ring also can be converted to a zwitterion, which would be of great interest in spite of lacking some function based on the nature of the unsubstituted imidazole ring. Two kinds of butyrates ($BuCO_2Et$ and $BuCO_2Bzl$) were selected not only as a model of an additional functionality but also as substituents that can be converted to carboxylic acids by deprotection. Among enzymes available for enzymatic polymerization, papain is often applied owing to its relatively broad substrate specificity. The papain-catalyzed polymerization of basic amino acids such as lysine as well as hydrophobic amino acids such as glycine and alanine was thoroughly investigated.[36,43−46] However, papain was not previously applied for the polymerization of His-containing monomers, although proteinase I- and proteinase K-catalyzed polymerization of His methyl or ethyl ester was reported.[39,40] This study addresses the papain-catalyzed polymerization of His-derived monomers and oligomeric units (Scheme 1).

Polymerization was initiated by the addition of papain to the pH-adjusted solutions of the monomers in phosphate buffer (pH 8), followed by incubation at 40 °C for 2 h. The results are listed in Table 1. Polymerization of the monomeric His derivatives His ethyl ester (His-OEt) and butyrated His ethyl ester (His(Bu)-OEt) did not afford any precipitate after the reaction (runs 1 and 2). The chemoenzymatic polymerization of hydrophobic amino acids such as alanine and leucine in an aqueous buffer usually results in a precipitate. In contrast, polyHis was soluble in an aqueous medium due to its hydrophilicity,[47] even if the chemoenzymatic polymerization of His-OEt underwent to afford oligoHis or polyHis. Therefore, each postpolymerization mixture was purified by ultrafiltration to remove the papain and desalted using pipette tips prepacked with the C18 stationary phase to isolate the polymerization medium-soluble part, including the unreacted monomer. The MALDI-TOF mass spectra of both extracted samples showed monomeric peaks but no peaks attributed to the oligomeric compounds, suggesting that polymerization of His-OEt and His(Bu)-OEt was not catalyzed by papain. This is probably due to the low affinity of the His residue for papain, which exhibits higher substrate specificity for aromatic and/or hydrophobic amino acids.

To improve the affinity of the monomer for papain, we conjugated a Gly residue to the His residue, which has been reported to enhance the affinity for papain.[33] Two types of His-containing dipeptide monomers with the Gly residue linked at the N- or C-terminus were designed. However, the conjugation of the Gly residue at the N-terminus (GlyHis-OEt and GlyHis(Bu)-OEt) did not improve the polymerizability of the His-containing dipeptide monomers (runs 3 and 4). On the other hand, Gly-conjugated dipeptides at the C-terminus (HisGly-OEt and His(Bu)Gly-OEt) polymerized well to afford white precipitates during polymerization (runs 5 and 6). These insoluble products were collected by centrifugation, washed with water, and then lyophilized to give white solids in 32 and 28% yields, respectively. A time course study of the polymerization of HisGly-OEt was performed at pH 8.0, 40 °C, and an initial monomer concentration of 1.0 M. The precipitate was rapidly formed within 30 min, and the yield of

https://doi.org/10.1021/acs.macromol.2c01036
Macromolecules 2022, 55, 6992−7002

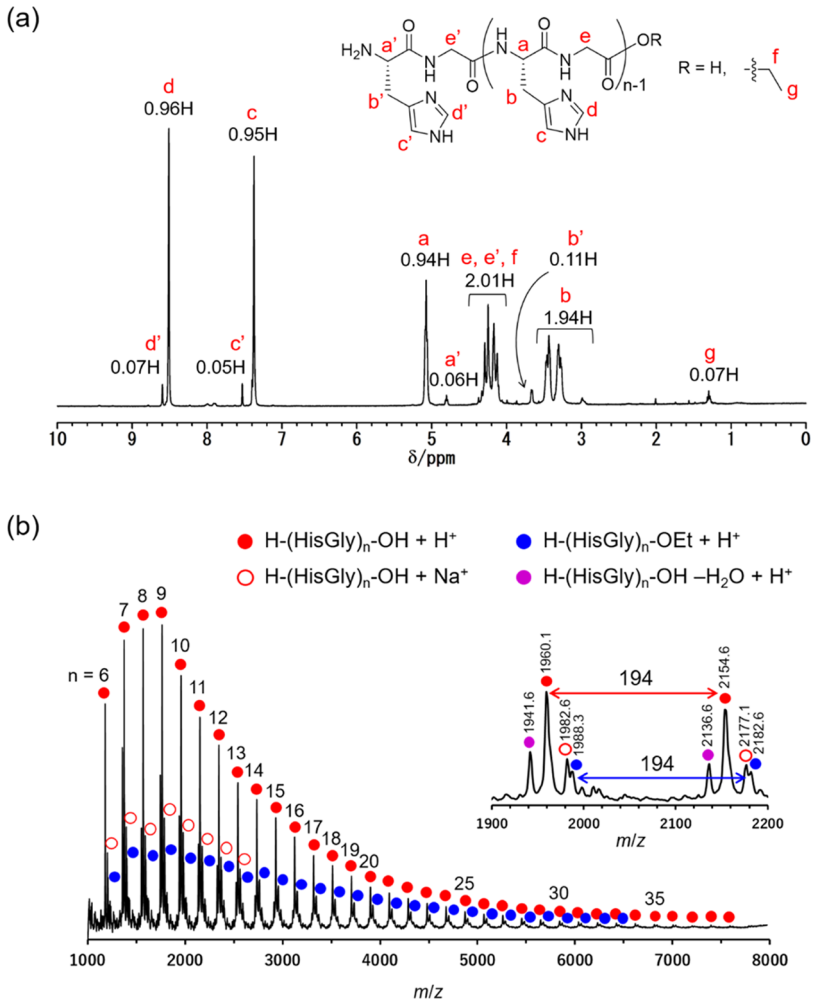

Figure 1. ^{1}H NMR (a) and MALDI-TOF mass (b) spectra of poly(HisGly) obtained by papain-catalyzed polymerization. TFA-*d* was used as a solvent for ^{1}H NMR.

the precipitate was gradually increased to a maximum after 2 h (Figure S20). On the other hand, prolonging the polymerization time to 4 h basically did not change the yield. This indicates that a 2 h reaction was enough to analyze the polymerization yield of His-containing monomers. The water-soluble part of each polymerization was also analyzed by ^{1}H NMR (Figure S21). The ethyl esters at the C-terminus of the monomer and/or the oligomer were found to be substantially hydrolyzed in 15 min. In addition, the proportion of the hydrolyzed C-terminus increased with time until 60 min. After 60 min, the ethyl esters were completely hydrolyzed. The C-terminus-hydrolyzed monomer and oligomer cannot be subjected to further polymerization. These results coincided with the results of the yield of the precipitate. Thus, the termination might occur via both the precipitation of products and the hydrolysis of ethyl ester groups of the monomers and oligomers. Both GlyHis and HisGly dipeptide monomers are expected to result in the same polypeptide with alternating sequences of His and Gly, but only the HisGly dipeptides provided the precipitate. These results indicate that the sequence of monomers is quite important for substrate recognition by the enzyme during polymerization. We also attempted the polymerization of His-containing tripeptides, namely, GlyHisGly derivatives with and without hydrophobic side chains on the imidazole ring. We have previously reported that sandwiching with Gly residues dramatically improved the polymerizability of nonproteinogenic amino acids by mitigating the low affinity for papain.[34,35] Similar to previous reports, the His-sandwiching tripeptide monomer GlyHisGly-OEt underwent polymerization to give a precipitate in a much higher yield at 1.0 M than dipeptide monomers (57%, run 7), whereas polymerization of GlyHisGly-OEt did not proceed at 0.10 M (run 8). A 10-fold concentration of papain at 0.10 M compared with that at 1.0 M might promote transamidation and/or hydrolysis of polymerized product in situ because poly(GlyHisGly) would be easily subjected to transamidation reaction as well as hydrolysis (described in detail later). In addition, poly(GlyHisGly) might suffer these side reactions for an extended period of time due to its higher water-solubility. These resulted in no precipitate when polymerized at the monomer concentration of 0.10 M.

To compare the effect of the substituents of His residues on polymerization, we applied a butyl group and two kinds of butyrate groups as side chains of the imidazole ring. We used the monomer concentration of 0.10 M for polymerization of the substituted monomers GlyHis(Bu)Gly-OEt, GlyHis-($BuCO_2Et$)Gly-OEt, and GlyHis($BuCO_2Bzl$)Gly-OEt because we had previously found that the highest yield was obtained at 0.10 M for polymerization of GlyHis(Bu)Gly-OEt.[38] All of the substituted monomers polymerized even at 0.10 M in yields

https://doi.org/10.1021/acs.macromol.2c01036
Macromolecules 2022, 55, 6992−7002

comparable to or higher than those of GlyHisGly-OEt at 1.0 M (54−70 and 57%). Papain has been reported to prefer amino acid residues bearing a large hydrophobic side chain at the P2 subsite position in its substrate pocket.[48] A similar tendency was observed in polymerization of the His-containing tripeptide series, except for polymerization of GlyHis(BuCO$_2$Bzl)Gly-OEt. For GlyHis(R)Gly-OEt, the yield of the precipitates increased in the following order: R = H < Bu < BuCO$_2$Et. This is in accordance with the order of hydrophobicity of the side chain on the imidazole ring of the His residue in the center of the tripeptide monomer. In addition, the precipitate yield for GlyHis(BuCO$_2$Bzl)Gly-OEt was the lowest among the four despite the presence of the largest hydrophobic side chain on the imidazole ring, implying that a hydrophobic side chain of suitable size exists at the P2 subsite of papain.

Chemical Characterization of the Resulting Polypeptides. ^{1}H NMR and MALDI-TOF MS measurements were conducted to characterize the chemical structures of the polypeptides. All precipitates were insoluble in common organic solvents, such as alcohols, dimethylformamide (DMF), dimethyl sulfoxide (DMSO), and pyridine, but were soluble in trifluoroacetic acid (TFA). Regarding the solubility, the ^{1}H NMR spectra of all of the precipitates were measured in TFA-*d*. The ^{1}H NMR and MALDI-TOF mass spectra of the precipitates obtained in the chemoenzymatic polymerization of HisGly-OEt are shown with their peak assignments as a typical example in Figure 1. In the ^{1}H NMR spectrum (Figure 1a), methylene protons of Gly residues were found at 4.05−4.20 ppm (e, e′). The signals assignable to the His residue at the N-terminus (a′, b′, c′, d′) were separated from those of the other His residues (a, b, c, d). The N-terminal α proton of the His residue (a′) was shifted downfield from the other His α protons (a), while methylene and imidazole protons of the N-terminal His residue (b′, c′, d′) were found upfield compared to the proton signals of the other His residues (b, c, d). These assignments proved that the precipitate generated during the chemoenzymatic polymerization of HisGly-OEt was poly(HisGly). The number-average degree of polymerization (DP$_n$) of poly(HisGly), the average number of HisGly sequences in the poly(HisGly) chains, was estimated to be 17.4 by the average of the integral ratios of protons c′ to c and d′ to d. In addition, the methyl proton of the ethyl ester group at the C-terminus appeared at 1.25 ppm (f). The integral ratio of the methyl proton should be 0.16, as calculated from the above-estimated DP$_n$ value, whereas the observed value was less than half of that (0.07), indicating that the hydrolysis of the ethyl ester group at the C-terminus occurred during papain-catalyzed polymerization. Moreover, the integral ratio of α protons of His residues (a′ and a) to α protons of Gly residues (e′ and e) was almost 0.5, suggesting the equal composition of Gly and His residues. The MALDI-TOF mass spectrum of poly(HisGly) mainly showed the three series of peaks derived from poly(HisGly) with ethyl ester or carboxylic acid terminal groups (Figure 1b). The peak-top degree of polymerization (DP$_{top}$) and the maximum degree of polymerization (DP$_{max}$) were 9 and 40, respectively. The appearance of the peaks of the C-terminal-hydrolyzed chain is consistent with the ^{1}H NMR results. On the other hand, there was no peak attributed to the His or Gly residue-defective polypeptides. Considering the equal composition suggested by ^{1}H NMR, the side reactions such as transamidation and hydrolysis of the peptide chain scarcely occurred in chemoenzymatic polymerization of HisGly-OEt, although the transamidation products were sometimes observed in chemoenzymatic polymerization of the di- or tripeptides containing Gly or Ala.[34,35] In addition, peaks attributed to the dehydration products of poly(HisGly) were observed, probably due to the formation of diketopiperazine and/or oxazolone at the C-terminus via protonation of the amide group of the His residue by imidazole.[49] The ^{1}H NMR and MALDI-TOF mass spectra of poly[His(Bu)Gly] are shown in Figure S22. No dehydration peak was observed for poly[His(Bu)Gly], suggesting that the dehydration peaks for poly(HisGly) could be attributed to the imidazole-catalyzed reaction.

The ^{1}H NMR spectra of all of the His-containing polypeptides obtained from tripeptide-type monomers (Figure S23) did not show the peak separation of N-terminal Gly and the other Gly residues, making the estimation of DP$_n$ by NMR impossible. In the MALDI-TOF mass spectrum (Figure S24), hydrolysis of the C-terminal ester was found to occur during polymerization. Also, the insertion of one to three Gly residues in poly(GlyHisGly) was detected. The insertion of one or two Gly residues in poly(GlyHisGly) was caused by the transamidation and/or the hydrolysis of poly(GlyHisGly), whereas the insertion of three excessive Gly residues in poly(GlyHisGly) indicated at least one transamidation side reaction along with the other transamidation and/or the hydrolysis. In the ^{1}H NMR spectrum of poly(GlyHisGly), the integral ratio of the α protons of Gly residues to those of His residues was 6.5, which is larger than the theoretical value of 4 for poly(GlyHisGly). These results suggest that irregular GlyGlyGly and GlyGlyGlyGly sequences should be included in poly(GlyHisGly) via transamidation. Transamidation and hydrolysis were sometimes observed in the chemoenzymatic polymerization of the di- or tripeptides containing Gly or Ala, which have a high affinity to papain.[34,35] Rapid chain propagation and product precipitation were reported to be important in minimizing or avoiding the transamidation reaction in polymerization of AlaGly-OEt.[32] The optimization of polymerization conditions such as the reaction pH, initial concentration of the monomer, and reaction time might suppress the transamidation side reactions to some extent, although complete suppression would be inherently unattainable. In contrast, considering that the integral ratio of α protons of Gly residues to those of His residues was almost 4 for His-substituted polypeptides, poly[GlyHis(R)Gly] (R = Bu, BuCO$_2$Et, BuCO$_2$Bzl), the polypeptides were confirmed to contain the periodic GlyHis(R)Gly sequence with negligible transamidation. The DP of poly(GlyHisGly) was lower than those of poly[GlyHis(Bu)Gly] and poly[GlyHis(BuCO$_2$Et)Gly]. Poly(GlyHisGly) might have relatively high solubility in aqueous media, which could cause enzymatic degradation of the polypeptide main chain by papain due to the longer contact time with papain. This situation was assumed to lead to a nonnegligible amount of transamidation, in contrast to the other His-substituted polypeptides. The DP of poly[GlyHis(BuCO$_2$Bzl)Gly] also decreased, probably due to its lower solubility in aqueous media, which was ascribed to the benzyl group, leading to precipitation in the early stage of polymerization.

Molecular Modeling Study of Monomers and Papain. As mentioned above, HisGly-OEt underwent polymerization, while GlyHis-OEt did not polymerize. To elucidate how such a large difference in the polymerization behavior arises when only the Gly-conjugated positions (N-terminus or C-terminus)

https://doi.org/10.1021/acs.macromol.2c01036
Macromolecules 2022, 55, 6992−7002

differ, we performed molecular docking simulations of GlyHis-OEt or HisGly-Oet to papain. The estimated free energies of binding in the best conformation for GlyHis-Oet and HisGly-OEt to the catalytic site of papain were −5.7 and −6.1 kcal mol^{-1}, respectively (Table 2). In addition, the second and

Table 2. Estimated Free Energies of Binding of GlyHis-OEt and HisGly-OEt to Papain and the Distances between the Thiol of Cysteine in the Catalytic Center of Papain and the Carbonyl of the Ester Group of Monomers

	GlyHis-OEt			HisGly-OEt	
mode	estimated $\Delta G_{binding}$ (kcal mol^{-1})	distance of S···C═O (Å)	mode	estimated $\Delta G_{binding}$ (kcal mol^{-1})	distance of S···C═O (Å)
1	−5.7	5.2	1	−6.1	1.8
2	−5.6	4.8	2	−5.7	0.9
3	−5.6	2.2	3	−5.7	0.9
4	−5.6	2.3	4	−5.6	2.4
5	−5.4	4.7	5	−5.5	0.7
6	−5.3	5.0	6	−5.5	3.8
7	−5.3	5.8	7	−5.5	2.4
8	−5.2	3.5	8	−5.5	1.7
9	−5.2	2.7	9	−5.5	0.8

subsequent binding energies ranged from −5.6 to −5.2 kcal mol^{-1} and from −5.7 to −5.5 kcal mol^{-1}, respectively. These results indicate that the two monomers did not have a substantially different affinity for papain. However, the binding direction of GlyHis-OEt was found to be opposite from that of HisGly-OEt in the most stable conformation (Figure 2). The ester moiety of the monomer was generally thioesterified by the thiol of the Cys residue in the catalytic triad of papain, leading to the activation of the monomer in papain-catalyzed polymerization. In the catalytic site of papain, the ethyl ester moiety of GlyHis-OEt was located apart from the Cys residue, whereas that of HisGly-OEt was located close to the Cys residue. The location difference of the ester group should result in the disparity in the polymerization behavior between the two monomers.

Molecular docking simulations of three tripeptide-based monomers, GlyHis(R)Gly-OEt (R = H, $BuCO_2Et$, $BuCO_2Bzl$), to papain were also carried out to examine the effect of the monomer side chain on the polymerization behavior. The estimated free energies of binding in the best conformation for GlyHis(R)Gly-OEt (R = H, $BuCO_2Et$, $BuCO_2Bzl$) to the catalytic site of papain were −6.5, −6.4, and −6.5 kcal mol^{-1}, respectively (Table S1). The second and subsequent binding energies were comparable, ranging from −6.2 to −5.7 kcal mol^{-1}, from −6.4 to −6.2 kcal mol^{-1}, and from −6.4 to −6.0 kcal mol^{-1}. Moreover, the arrangements of the monomers in the catalytic site of papain were similar to each other, in contrast to dipeptide-based monomers (Figure S25). These results indicate that the hydrophobic side chain of the tripeptide monomers did not greatly affect the affinity for the catalytic site of papain. Namely, the molecular docking simulation suggests that the polymerizability of tripeptide monomers on the chemoenzymatic polymerization is similar. Therefore, the decrease in the yield and DPs in poly[GlyHis-($BuCO_2Bzl$)Gly] could be attributed to precipitation in the early stage of polymerization due to hydrophobicity, not the catalytic activity of papain.

Secondary Structure of the His-Containing Polypeptides. WAXD analysis of the obtained His-containing polypeptides was performed except for poly(GlyHisGly), which includes a random sequence to some extent caused by transamidation (Figure 3). Several strong diffraction peaks

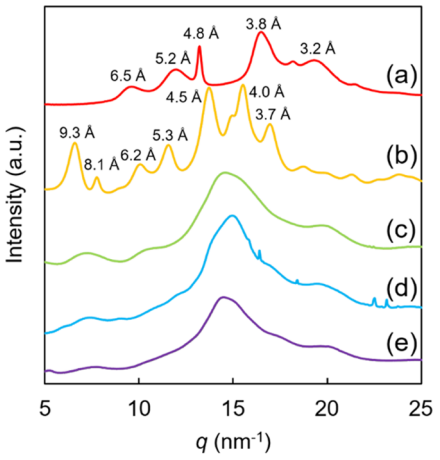

Figure 3. 1D WAXD profiles of poly(HisGly) (a), poly[His(Bu)Gly] (b), poly[GlyHis(Bu)Gly] (c), poly[GlyHis($BuCO_2Et$)Gly] (d), and poly[GlyHis($BuCO_2Bzl$)Gly] (e) in the solid state.

were detected for the dipeptide-based polypeptides (poly-(HisGly) and poly[His(Bu)Gly]), while broad amorphous peaks were observed for the tripeptide-based polypeptides (poly-GlyHis(R)Gly, R = Bu, $BuCO_2Et$, $BuCO_2Bzl$). Judging from the sharpness of the peaks, the crystallinity of the dipeptide-based polypeptides seems to be higher than that of the tripeptide-based polypeptides, which indicates the ordered structure for the dipeptide-based polypeptides. The crystallinity of the polypeptides were calculated by peak separations of the WAXD profiles to be 41.6, 50.2, 29.3, 19.6, and 30.7% for poly(HisGly), poly[His(Bu)Gly], poly[GlyHis(Bu)Gly],

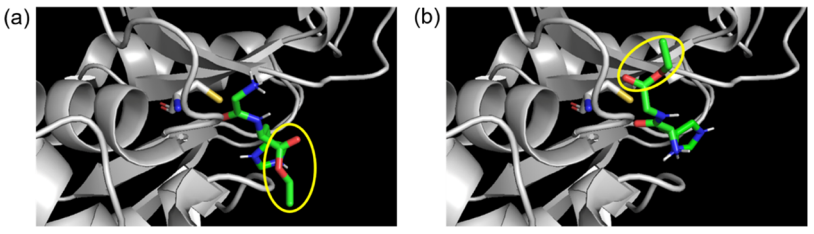

Figure 2. Best binding conformations of GlyHis-OEt (a) and HisGly-OEt (b) to the catalytic site of papain. Papain is displayed as a gray cartoon. The sulfur atom of the Cys25 catalytic residue is shown as a deep yellow stick representation, and the ester group of the monomer is circled in yellow.

https://doi.org/10.1021/acs.macromol.2c01036
Macromolecules 2022, 55, 6992−7002

poly[GlyHis(BuCO$_2$Et)Gly], and poly[GlyHis(BuCO$_2$Bzl)-Gly], respectively (Figure S26).

The FT-IR spectra of the polypeptides were also measured to investigate the secondary structure in the solid state (Figure 4). The strong absorption bands exhibited in the amide I region were attributed to the carbonyl stretching vibration of the amide group in the main chain for all the polypeptides. In addition, absorption bands attributed to the carbonyl stretching vibration of the ester group in the side chain were observed for poly[GlyHis(BuCO$_2$Et)Gly] and poly[GlyHis-(BuCO$_2$Bzl)Gly]. Poly(HisGly) showed amide I absorption at 1631 cm^{-1}, which reveals that poly(HisGly) forms a β-sheet structure.[50−53] On the other hand, the other polypeptides showed peaks at 1649 and 1656 cm^{-1}, which were assignable to α-helical and/or random structures. Combined with the WAXD data, the tripeptide-based polypeptides predominantly adopted a random structure. A periodically repeating sequence of HisGly promoted the formation of a β-sheet structure via a precise hydrogen-bonding pattern between polypeptide strands for poly(HisGly). On the other hand, the substitution of a large hydrophobic side chain on the imidazole ring of the His residue might disturb the hydrogen bonding between polypeptide strands to form a random structure for the other polypeptides despite the periodic HisGly or GlyHisGly sequences.

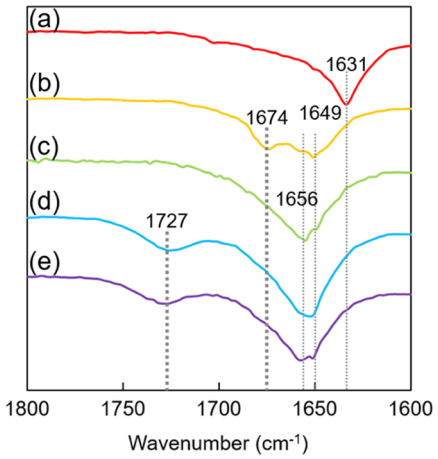

Figure 4. IR spectra of poly(HisGly) (a), poly[His(Bu)Gly] (b), poly[GlyHis(Bu)Gly] (c), poly[GlyHis(BuCO$_2$Et)Gly] (d), and poly[GlyHis(BuCO$_2$Bzl)Gly] (e) in the solid state.

Thermal Properties of the His-Containing Polypeptides. Thermogravimetric analysis (TGA) and differential scanning calorimetry (DSC) were applied to elucidate the thermal properties of the His-containing polypeptides (Figure 5). Poly(HisGly) showed the highest 5% degradation temperature (T_{d5}, 256 °C) (Figure 5b), probably due to the formation of a β-sheet structure. The T_{d5} values of the other polypeptides ranged from 230 to 248 °C. Poly[GlyHis(BuCO$_2$Bzl)Gly] had the lowest thermal stability, which might be attributed to the low molecular weight of the polypeptide. PolyHis was reported to show an endothermic peak ascribed to thermal decomposition at 181 °C by differential thermal analysis.[54] The periodic introduction of Gly residues increased the thermal stability of His-containing polypeptides even though their molecular weights were not very high. In the DSC curves, no transition temperature was detected for poly(HisGly) and poly[His(Bu)Gly], whereas a glass transition temperature (T_g) was observed for poly[GlyHis(Bu)Gly] and poly[GlyHis-(BuCO$_2$Bzl)Gly] (120 °C and 76 °C, respectively) (Figure 6). Although common polypeptides, including polyGly and polyLeu, exhibit no phase transition, the incorporation of aromatic rings or aliphatic chains into the polypeptide backbone has been reported to induce a glass transition.[36,46] We found that the introduction of a flexible alkyl chain into the

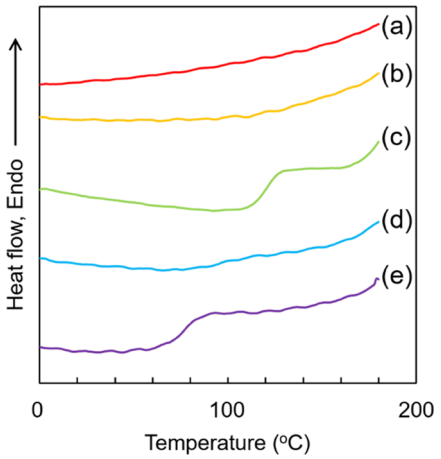

Figure 6. DSC profiles in the second heating run (20 °C min^{-1}) of poly(HisGly) (a), poly[His(Bu)Gly] (b), poly[GlyHis(Bu)Gly] (c), poly[GlyHis(BuCO$_2$Et)Gly] (d), and poly[GlyHis(BuCO$_2$Bzl)Gly] (e).

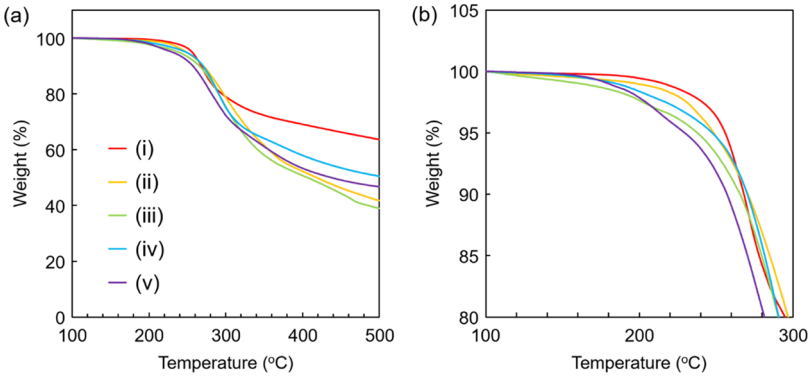

Figure 5. (a) Thermograms of TGA (20 °C min^{-1}) (a) and enlarged view from 100 to 300 °C (b) of poly(HisGly) (i), poly[His(Bu)Gly] (ii), poly[GlyHis(Bu)Gly] (iii), poly[GlyHis(BuCO$_2$Et)Gly] (iv), and poly[GlyHis(BuCO$_2$Bzl)Gly] (v).

https://doi.org/10.1021/acs.macromol.2c01036
Macromolecules 2022, 55, 6992−7002

functional group of polypeptide side chains would be an alternative design to afford polypeptides that show a glass transition before decomposition.

CONCLUSIONS

We demonstrated that papain-catalyzed polymerization of His-containing dipeptide ethyl esters [GlyHis(R)-OEt and His(R)Gly-OEt, R = H or Bu] proceeded in a sequence-dependent manner: His(R)Gly-OEt was well polymerized, while GlyHis(R)-OEt did not undergo polymerization. The obtained polypeptides had a distinct alternating sequence of HisGly residues. A docking simulation study between dipeptide monomers and papain revealed that the HisGly-based monomer adopted a conformation more likely to react with the catalytic center of papain, supporting the difference in the polymerizability of the dipeptide monomers. GlyHis(R)-Gly-OEt (R = H, Bu, $BuCO_2Et$, or $BuCO_2Bzl$) was also polymerized well to afford the periodic His-containing polypeptides. The MALDI-TOF mass and ^1H NMR spectra revealed that the His-containing polypeptides with distinct periodic sequence structures were obtained with their C-termini partly hydrolyzed except in polymerization of GlyHisGly-OEt, where transamidation caused the random insertion of additional Gly residues. Polymerization proceeded well regardless of the side chain modification, and the DP_{max} of the obtained His-containing polypeptides was up to 39 for polymerization of HisGly-OEt, which afford a degree of polymerization of the highest peak (DP_{top}) of 9 in the MALDI-TOF mass spectrum and a DP_n of 17.4. The structural characterization of the obtained His-containing polypeptides using IR spectroscopy and WAXD indicated that the β-sheet structure formed for poly(HisGly), whereas more amorphous structures formed for the other polypeptides. Poly(HisGly) exhibited the highest thermal stability among all of the obtained HisGly- and GlyHisGly-based polypeptides, reflecting the difference in secondary structures ascribed to their sequences. The results of chemoenzymatic synthesis of periodic His-containing polypeptides with high molecular weights in a sequence-dependent manner will provide new insight into the rational design and synthesis of periodic polypeptides, potentially enabling the use of polypeptide materials in various applications.

ASSOCIATED CONTENT

Supporting Information

The Supporting Information is available free of charge at https://pubs.acs.org/doi/10.1021/acs.macromol.2c01036.

Detailed experimental procedures for monomer syntheses, ^1H NMR spectra of monomers, ^1H NMR spectra of the His-containing polypeptides, MALDI-TOF mass spectra of the His-containing polypeptides, best binding conformation by docking simulation, and estimated free energy on the docking simulation of the GlyHisGly-based monomers to papain (PDF)

AUTHOR INFORMATION

Corresponding Authors

Kousuke Tsuchiya − *Department of Material Chemistry, Graduate School of Engineering, Kyoto University, Nishikyo-ku, Kyoto 615-8510, Japan;* orcid.org/0000-0003-2364-8275; Email: tsuchiya.kosuke.3n@kyoto-u.ac.jp

Keiji Numata − *Department of Material Chemistry, Graduate School of Engineering, Kyoto University, Nishikyo-ku, Kyoto 615-8510, Japan; Biomacromolecules Research Team, RIKEN Center for Sustainable Resource Science, Wako, Saitama 351-0198, Japan;* orcid.org/0000-0003-2199-7420; Email: numata.keiji.3n@kyoto-u.ac.jp

Authors

Kayo Terada − *Department of Material Chemistry, Graduate School of Engineering, Kyoto University, Nishikyo-ku, Kyoto 615-8510, Japan*

Taichi Kurita − *Department of Material Chemistry, Graduate School of Engineering, Kyoto University, Nishikyo-ku, Kyoto 615-8510, Japan*

Joan Gimenez-Dejoz − *Biomacromolecules Research Team, RIKEN Center for Sustainable Resource Science, Wako, Saitama 351-0198, Japan;* orcid.org/0000-0002-3839-950X

Hiroyasu Masunaga − *Japan Synchrotron Radiation Research Institute, Sayo-gun, Hyogo 679-5198, Japan*

Complete contact information is available at: https://pubs.acs.org/10.1021/acs.macromol.2c01036

Author Contributions

K.Tsuchiya and K.N. conceived and designed the research. K.Terada, T.K., J.G.D., and H.M. performed the experiments and analyzed the data. K.Terada wrote the manuscript, and K.Tsuchiya and K.N. edited the manuscript.

Funding

This work was supported by Grants-in-Aid from JST ERATO Grant No. JPMJER1602, JST PRESTO Grant No. JPMJPR21N6, Grant-in-Aid for Transformative Research Areas (B) Grant No. JP20H05735, and JSPS KAKENHI Grant Nos. JP20K05636 and JP20K05718. This work was partially supported by Asahi Glass Foundation.

Notes

The authors declare no competing financial interest.

REFERENCES

(1) Ramakers, B. E. I.; van Hest, J. C. M.; Löwik, D. W. P. M. Molecular tools for the construction of peptide-based materials. *Chem. Soc. Rev.* **2014**, *43*, 2743−2756.

(2) Pepe-Mooney, B. J.; Fairman, R. Peptides as materials. *Curr. Opin. Struct. Biol.* **2009**, *19*, 483−494.

(3) Numata, K. Poly(amino acid)s/polypeptides as potential functional and structural materials. *Polym. J.* **2015**, *47*, 537−545.

(4) Ulijn, R. V.; Smith, A. M. Designing peptide based nanomaterials. *Chem. Soc. Rev.* **2008**, *37*, 664−675.

(5) Harrington, M. J.; Fratzl, P. Natural load-bearing protein materials. *Prog. Mater. Sci.* **2021**, *120*, No. 100767.

(6) Numata, K. *Biopolymer Science for Proteins and Peptides*; Elsevier, 2021.

(7) McGaughey, G. B.; Gagné, M.; Rappé, A. K. π-Stacking interactions. Alive and well in proteins. *J. Biol. Chem.* **1998**, *273*, 15458−15463.

(8) Liao, S.-M.; Du, Q.-S.; Meng, J.-Z.; Pang, Z.-W.; Huang, R.-B. The multiple roles of histidine in protein interactions. *Chem. Cent. J.* **2013**, *7*, No. 44.

(9) Christianson, D. W.; Alexander, R. S. Carboxylate-histidine-zinc interactions in protein structure and function. *J. Am. Chem. Soc.* **1989**, *111*, 6412−6419.

(10) Hatip Koc, M.; Cinar Ciftci, G.; Baday, S.; Castelletto, V.; Hamley, I. W.; Guler, M. O. Hierarchical Self-Assembly of Histidine-Functionalized Peptide Amphiphiles into Supramolecular Chiral Nanostructures. *Langmuir* **2017**, *33*, 7947−7956.

(11) Lointier, M.; Aisenbrey, C.; Marquette, A.; Tan, J. H.; Kichler, A.; Bechinger, B. Membrane pore-formation correlates with the hydrophilic angle of histidine-rich amphipathic peptides with multiple biological activities. *Biochim. Biophys. Acta, Biomembr.* **2020**, *1862*, No. 183212.
(12) Schneider, F. Histidine in enzyme active centers. *Angew. Chem., Int. Ed.* **1978**, *17*, 583−592.
(13) Bachovchin, W. W.; Wong, W. Y. L.; Farr-Jones, S.; Shenvi, A. B.; Kettner, C. A. Nitrogen-15 NMR spectroscopy of the catalytic-triad histidine of a serine protease in peptide boronic acid inhibitor complexes. *Biochemistry* **1988**, *27*, 7689−7697.
(14) Markley, J. L.; Westler, W. M. Protonation-State Dependence of Hydrogen Bond Strengths and Exchange Rates in a Serine Protease Catalytic Triad: Bovine Chymotrypsinogen A. *Biochemistry* **1996**, *35*, 11092−11097.
(15) Vernet, T.; Tessier, D. C.; Chatellier, J.; Plouffe, C.; Lee, T. S.; Thomas, D. Y.; Storer, A. C.; Ménard, R. Structural and functional roles of asparagine 175 in the cysteine protease papain. *J. Biol. Chem.* **1995**, *270*, 16645−16652.
(16) Zhang, L.; Xu, J.; Wang, F.; Ding, Y.; Wang, T.; Jin, G.; Martz, M.; Gui, Z.; Ouyang, P.; Chen, P. Histidine-Rich Cell-Penetrating Peptide for Cancer Drug Delivery and Its Uptake Mechanism. *Langmuir* **2019**, *35*, 3513−3523.
(17) Lee, H. J.; Huang, Y. W.; Chiou, S. H.; Aronstam, R. S. Polyhistidine facilitates direct membrane translocation of cell-penetrating peptides into cells. *Sci. Rep.* **2019**, *9*, No. 9398.
(18) Kimura, S.; Kawano, T.; Iwasaki, T. Short polyhistidine peptides penetrate effectively into Nicotiana tabacum-cultured cells and Saccharomyces cerevisiae cells. *Biosci., Biotechnol., Biochem.* **2017**, *81*, 112−118.
(19) Midoux, P.; Pichon, C.; Yaouanc, J. J.; Jaffrès, P. A. Chemical vectors for gene delivery: a current review on polymers, peptides and lipids containing histidine or imidazole as nucleic acids carriers. *Br. J. Pharmacol.* **2009**, *157*, 166−178.
(20) Kichler, A.; Leborgne, C.; März, J.; Danos, O.; Bechinger, B. Histidine-rich amphipathic peptide antibiotics promote efficient delivery of DNA into mammalian cells. *Proc. Natl. Acad. Sci. U.S.A.* **2003**, *100*, 1564−1568.
(21) Kim, G. M.; Bae, Y. H.; Jo, W. H. pH-induced Micelle Formation of Poly(histidine-co-phenylalanine)-block-Poly(ethylene glycol) in Aqueous Media. *Macromol. Biosci.* **2005**, *5*, 1118−1124.
(22) Park, W.; Kim, D.; Kang, H. C.; Bae, Y. H.; Na, K. Multi-arm histidine copolymer for controlled release of insulin from poly(lactide-co-glycolide) microsphere. *Biomaterials* **2012**, *33*, 8848−8857.
(23) Bilalis, P.; Varlas, S.; Kiafa, A.; Velentzas, A.; Stravopodis, D.; Iatrou, H. Preparation of hybrid triple-stimuli responsive nanogels based on poly(L-histidine). *J. Polym. Sci., Part A: Polym. Chem.* **2016**, *54*, 1278−1288.
(24) Johnson, R. P.; Jeong, Y.-I.; Choi, E.; Chung, C.-W.; Kang, D. H.; Oh, S.-O.; Suh, H.; Kim, I. Biocompatible Poly(2-hydroxyethyl methacrylate)-b-poly(L-histidine) Hybrid Materials for pH-Sensitive Intracellular Anticancer Drug Delivery. *Adv. Funct. Mater.* **2012**, *22*, 1058−1068.
(25) Qin, X.; Xie, W.; Su, Q.; Du, W.; Gross, R. A. Protease-Catalyzed Oligomerization of l-Lysine Ethyl Ester in Aqueous Solution. *ACS Catal.* **2011**, *1*, 1022−1034.
(26) Fukuoka, T.; Tachibana, Y.; Tonami, H.; Uyama, H.; Kobayashi, S. Enzymatic Polymerization of Tyrosine Derivatives. Peroxidase- and Protease-Catalyzed Synthesis of Poly(tyrosine)s with Different Structures. *Biomacromolecules* **2002**, *3*, 768−774.
(27) Narai-Kanayama, A.; Hanaishi, T.; Aso, K. α-Chymotrypsin-catalyzed synthesis of poly-l-cysteine in a frozen aqueous solution. *J. Biotechnol.* **2012**, *157*, 428−436.
(28) Numata, K.; Baker, P. J. Synthesis of Adhesive Peptides Similar to Those Found in Blue Mussel (Mytilus edulis) Using Papain and Tyrosinase. *Biomacromolecules* **2014**, *15*, 3206−3212.
(29) Ma, Y.; Sato, R.; Li, Z.; Numata, K. Chemoenzymatic Synthesis of Oligo(l-cysteine) for Use as a Thermostable Bio-Based Material. *Macromol. Biosci.* **2016**, *16*, 151−159.
(30) Watanabe, T.; Terada, K.; Takemura, S.; Masunaga, H.; Tsuchiya, K.; Lamprou, A.; Numata, K. Chemoenzymatic Polymerization of l-Serine Ethyl Ester in Aqueous Media without Side-Group Protection. *ACS Polym. Au* **2022**, *2*, 147−156.
(31) Tsuchiya, K.; Numata, K. Chemoenzymatic Synthesis of Polypeptides for Use as Functional and Structural Materials. *Macromol. Biosci.* **2017**, *17*, No. 1700177.
(32) Qin, X.; Khuong, A. C.; Yu, Z.; Du, W.; Decatur, J.; Gross, R. A. Simplifying alternating peptide synthesis by protease-catalyzed dipeptide oligomerization. *Chem. Commun.* **2013**, *49*, 385−387.
(33) Gudeangadi, P. G.; Tsuchiya, K.; Sakai, T.; Numata, K. Chemoenzymatic synthesis of polypeptides consisting of periodic di- and tri-peptide motifs similar to elastin. *Polym. Chem.* **2018**, *9*, 2336−2344.
(34) Tsuchiya, K.; Numata, K. Chemoenzymatic synthesis of polypeptides containing the unnatural amino acid 2-aminoisobutyric acid. *Chem. Commun.* **2017**, *53*, 7318−7321.
(35) Gudeangadi, P. G.; Uchida, K.; Tateishi, A.; Terada, K.; Masunaga, H.; Tsuchiya, K.; Miyakawa, H.; Numata, K. Poly(alanine-nylon-alanine) as a bioplastic: chemoenzymatic synthesis, thermal properties and biological degradation effects. *Polym. Chem.* **2020**, *11*, 4920−4927.
(36) Tsuchiya, K.; Kurokawa, N.; Gimenez-Dejoz, J.; Gudeangadi, P. G.; Masunaga, H.; Numata, K. Periodic introduction of aromatic units in polypeptides via chemoenzymatic polymerization to yield specific secondary structures with high thermal stability. *Polym. J.* **2019**, *51*, 1287−1298.
(37) Zhou, J.; Li, Y.; Dong, H.; Yuan, H.; Ren, T.; Li, Y. Effect of monomer sequence of poly(histidine/lysine) catiomers on gene packing capacity and delivery efficiency. *RSC Adv.* **2015**, *5*, 14138−14146.
(38) Tsuchiya, K.; Yilmaz, N.; Miyamoto, T.; Masunaga, H.; Numata, K. Zwitterionic Polypeptides: Chemoenzymatic Synthesis and Loosening Function for Cellulose Crystals. *Biomacromolecules* **2020**, *21*, 1785−1794.
(39) Grindy, S. C.; Lenz, M.; Holten-Andersen, N. Engineering Elasticity and Relaxation Time in Metal-Coordinate Cross-Linked Hydrogels. *Macromolecules* **2016**, *49*, 8306−8312.
(40) Dannenberg, A. M., Jr.; Smith, E. L. Action of proteinase I of bovine lung; hydrolysis of the oxidized B chain of insulin; polymer formation from amino acid esters. *J. Biol. Chem.* **1955**, *215*, 55−66.
(41) Trott, O.; Olson, A. J. AutoDock Vina: Improving the speed and accuracy of docking with a new scoring function, efficient optimization, and multithreading. *J. Comput. Chem.* **2010**, *31*, 455−461.
(42) Pickersgill, R. W.; Harris, G. W.; Garman, E. Structure of monoclinic papain at 1.60 A resolution. *Acta Crystallogr., Sect. B: Struct. Sci.* **1992**, *48*, 59−67.
(43) Baker, P. J.; Numata, K. Chemoenzymatic synthesis of poly (L-alanine) in aqueous environment. *Biomacromolecules* **2012**, *13*, 947−951.
(44) Ageitos, J. M.; Yazawa, K.; Tateishi, A.; Tsuchiya, K.; Numata, K. The benzyl ester group of amino acid monomers enhances substrate affinity and broadens the substrate specificity of the enzyme catalyst in chemoenzymatic copolymerization. *Biomacromolecules* **2016**, *17*, 314−323.
(45) Fagerland, J.; Finne-Wistrand, A.; Numata, K. Short one-pot chemo-enzymatic synthesis of L-lysine and L-alanine diblock co-oligopeptides. *Biomacromolecules* **2014**, *15*, 735−743.
(46) Yazawa, K.; Gimenez-Dejoz, J.; Masunaga, H.; Hikima, T.; Numata, K. Chemoenzymatic synthesis of a peptide containing nylon monomer units for thermally processable peptide material application. *Polym. Chem.* **2017**, *8*, 4172−4176.
(47) Ma, Y.; Li, Z.; Numata, K. Synthetic Short Peptides for Rapid Fabrication of Monolayer Cell Sheets. *ACS Biomater. Sci. Eng.* **2016**, *2*, 697−706.
(48) Florence, M.; Ezekiel, A. Papain, a Plant Enzyme of Biological Importance: A Review. *Am. J. Biochem. Biotechnol.* **2012**, *8*, 99−104.

https://doi.org/10.1021/acs.macromol.2c01036
Macromolecules 2022, 55, 6992−7002

(49) Knapp-Mohammady, M.; Young, A. B.; Paizs, B.; Harrison, A. G. Fragmentation of doubly-protonated Pro-His-Xaa tripeptides: formation of b(2)(2+) ions. *J. Am. Soc. Mass Spectrom.* **2009**, *20*, 2135−2143.
(50) Hu, X.; Kaplan, D.; Cebe, P. Determining Beta-Sheet Crystallinity in Fibrous Proteins by Thermal Analysis and Infrared Spectroscopy. *Macromolecules* **2006**, *39*, 6161−6170.
(51) Tretinnikov, O. N.; Tamada, Y. Influence of Casting Temperature on the Near-Surface Structure and Wettability of Cast Silk Fibroin Films. *Langmuir* **2001**, *17*, 7406−7413.
(52) Teramoto, H.; Miyazawa, M. Molecular Orientation Behavior of Silk Sericin Film as Revealed by ATR Infrared Spectroscopy. *Biomacromolecules* **2005**, *6*, 2049−2057.
(53) Dong, A.; Huang, P.; Caughey, W. S. Protein secondary structures in water from second-derivative amide I infrared spectra. *Biochemistry* **1990**, *29*, 3303−3308.
(54) Yamada, M.; Moritani, Y. Polypeptide for anhydrous proton conductor. *Electrochim. Acta* **2014**, *144*, 168−173.

https://doi.org/10.1021/acs.macromol.2c01036
Macromolecules 2022, 55, 6992−7002